

ANALYSIS OF THE TEMPERATURE DISTRIBUTIONS OF BOULDERS ON C-TYPE ASTEROID 162173 RYUGU OBSERVED IN LOW ALTITUDE OPERATION OF THE ASTEROID EXPLORER HAYABUSA2., Ayumu Ohsugi^{1,2}, Naoya Sakatani³, Yuri Shimaki¹, Masanori Kanamaru¹, Hiroki Senshu⁴, Takehiko Arai⁵, Hirohide Demura⁶, Toru Kouyama⁷, Tomohiko Sekiguchi⁸, Satoshi Tanaka^{1,2}, and Tatsuaki Okada^{1,2}, ¹The University of Tokyo (a.ohsugi@chem.s.u-tokyo.ac.jp), Japan, ²Japan Aerospace Exploration Agency, Sagami-hara, Japan, ³Rikkyo University, Tokyo, Japan, ⁴Chiba Institute of Technology, Japan, ⁵Maebashi Institute of Technology, Japan, ⁶University of Aizu, Japan, ⁷National Institute of Advanced Industrial Science and Technology, Tokyo, Japan, ⁸Hokkaido University of Education, Asahikawa, Japan.

Introduction: The asteroid explorer Hayabusa2 [1] has the Thermal Infrared Imager (TIR) [2,3] which obtained the digital thermal images to indicate the thermal radiation from C-type asteroid 162173 Ryugu. In this study, to obtain detailed thermal properties of boulders at Ryugu, we analyzed TIR images taken below the altitude of 500 m and investigated temperature variations of boulders taken with more than 100 pixels and their physical state in the specific regions.

Observation Conditions: TIR has a field of view (FOV) of $16.7^\circ \times 12.7^\circ$ and the effective pixels of the detector of 328×248 , resulting in the spatial resolution about of 0.051° per pixel [2]. A temperature range which TIR covers is 150 to 460 K and the well-calibrated temperature range is 230 to 420 K. We used TIR images taken during the release paths for the MINERVA rover (MNRV) on 21st September 2018, and the MASCOT lander (MSCT), on 3rd October 2018 1st touchdown (TD1-L08E1) on 21st February 2019, and the touchdown rehearsals (TD1-R1A) on 15th October 2018.

Results and Discussions: Total numbers of detected boulders were 355 (MNRV), 312 (MSCT), 368 (TD1-L08E1), and 311 (TD1-R1A). Also, the detection errors were obtained as $\pm 5.2\%$ (MNRV), $\pm 5.5\%$ (MSCT), $\pm 5.1\%$ (TD1-L08E1), and $\pm 5.6\%$ (TD1-R1A) by Wald inequality [4]. In terms of the maximum temperature distribution, the values of full width at half maximum (FWHM) of MNRV, MSCT, TD1-L08E1, and TD1-R1A were 11.0 ± 0.49 (K), 13.6 ± 0.68 (K), 13.4 ± 0.44 (K), and 11.5 ± 0.84 (K), respectively. FWHM allows us to infer a variety of thermophysical and thermochemical properties of boulders. From the FWHM values, it was suggested that the boulders of MSCT and TD1-L08E1 showed wider varieties of thermal inertias than those of MNRV and TD1-R1A. In addition, from Figure 1 (a), the widths of the temperature change distribution curves of average temperature were about the same as those of maximum in all regions, so the influence of the shadows of the boulders on the average temperature distributions was limited. Moreover, from the normal Q-Q plots shown in Figure 1 (b), where the x-axis is the observed value and the y-axis is the expected value which is assumed

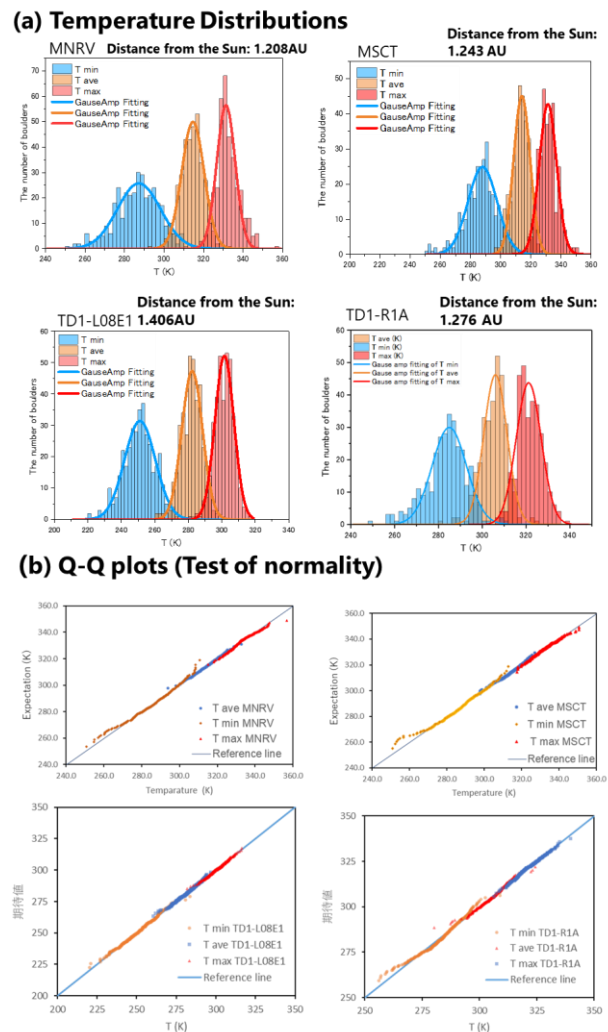


Figure1: Temperature distributions (a) and Q-Q plots (b)

the detected value follows a normal distribution, the temperatures could follow the normal distribution. It is considered that the temperatures of boulders were different due to the variation in the geometric shape of the boulder surface and the difference in the structure inside the boulders. Furthermore, the calculated slopes of the size-frequency distributions (SFD) divided by measured altitudes were in the range of -4.38 to -0.36 and these values were consistent with those investigat-

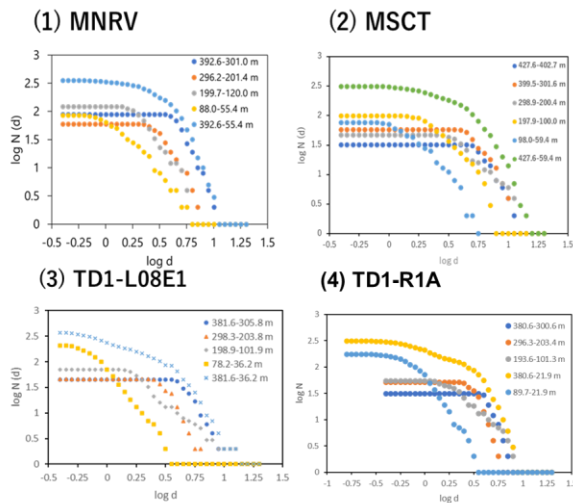


Figure 2: Size-Frequency distributions of boulders (SFD) in the observation areas

ed by Michikami T *et al.*, (2019) [6], who suggested the existence of boulders formed when Ryugu's parent body was destroyed and those covered with regolith layers. However, it should be noted that the SFD value may be calculated low due to the influence of the small number of plots. Moreover, in order to obtain further properties, we calculated thermal inertias using the average values of maximum temperatures of boulders. Due to the geometrical differences in the surface of the boulders, shadows have existed on the surface layer, and the average temperature of the boulders was underestimated, and the calculation was divergent and difficult to determine in the case of low temperatures. As a result of calculation, the range of thermal inertias [7] was calculated as low as 198.5 to 299.1 [$\text{J m}^{-2} \text{s}^{-0.5} \text{K}^{-1}$ (hereafter, tiu)] with the one-dimensional heat diffusion equation [8]. Figure 3 represents the temperature profiles of the boulder surface and the values of thermal inertia. Our results are consistent with that of the global average estimated as 225 ± 45 tiu by Shimaki *et al.* (2020) [9] and are higher than that of a high-temperature boulder assembly (HS1) as 73 ± 25 tiu reported by Sakatani *et al.*, (2021) [10]. As the porous and fluffy material has low thermal inertia, the boulders were considered to be porous compared with typical carbonaceous chondrite meteorites. In this study, we assumed that the surfaces of boulders were confronted to the images so that further detailed study considering the surface local slopes is needed to estimate more accurately. When considering the surface roughness of boulders, the amount of solar energy flux reaching them is changed, and there is some potential difference in the derived thermal inertia.

Summary and Future works: The total numbers of detected boulders were 355 (MNRV), 312 (MSCT),

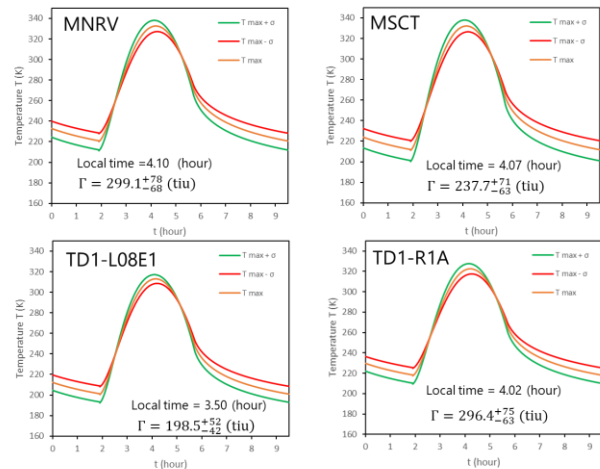


Figure 3: the temperature profiles of the boulder surface and the values of thermal inertia

368 (TD1-L08E1), and 311 (TD1-R1A) and the normal Q-Q plots suggested that the average temperature distributions of boulders were close to the normal distribution. The reason why temperature distributions were diverse is that the temperatures of boulders were different due to the variation in the geometric shape of the boulder surface and the difference in the structure inside the boulders. Moreover, the values of slopes of SFD and thermal inertias suggested the existence of boulders formed when Ryugu's parent body was destroyed, boulders covered with regolith layers, and porous and fluffy boulders. In the future, we plan to investigate the areas, which have not been fully investigated (DO-S01: Decent operation for S01), as well as the details of boulders, which are extremely hot and cold compared to others.

Acknowledgments: The authors appreciate Drs. Koji Matsumoto and Kyoko Yamamoto at the National Astronomical Observatory of Japan for the use of the LIDAR corrected trajectory of the Hayabusa2 spacecraft. This study is partly supported by the JSPS Kakenhi No. JP17H06459 (Aqua Planetology).

References: [1] Watanabe S. *et al.*, *Science* **364**, 268-272 (2019), [2] Okada, T. *et al.*, *Space Sci. Rev.*, **208**, 255-286 (2017), [3] Okada, T. *et al.*, *Nature* **579**, 518-522 (2020), [4] Kurihara, S., *Introduction to statistics: from testing to multivariate analysis and experimental design*, Ohmsha Ltd., pp.336 (2011), [5] Walsh *et al.*, *Nature* **454**, 188-191 (2008), [6] Michikami, T *et al.*, *Icarus* **331**, 179-191(2019), [7] Okada, T. *et al.*, 13th Space Science Symposium, ISAS/JAXA, P2-117 (2013), [8] Takita, J. *et al.*, *Space Sci Rev*, **208**, 287-315 (2017), [9] Shimaki Y. *et al.*, *Icarus* **348**, 113835 (2020). [10] Sakatani N. *et al.*, *Nature Astronomy*, **vol5** 766-774 (2021).